Rev.Adv.Mater.Sci. 20(2009) 77-84

CONFOCAL RAMAN MICROSCOPY: NON-DESTRUCTIVE MATERIALS ANALYSIS WITH MICROMETER RESOLUTION

Kerim R. Allakhverdiev[1,4], Deliani Lovera[2], Volker Altstädt[2], Philipp Schreier[3] and Lothar Kador[3]

[1]Marmara Research Centre of TÜBITAK, Materials Institute, P.K. 21 TR-41470 Gebze/Koçaeli, Turkey
[2] Department of Polymer Engineering, University of Bayreuth, D-95440 Bayreuth, Germany
[3] Institute of Physics and Bayreuther Institut für Makromolekülforschung (BIMF), University of Bayreuth, D-95440 Bayreuth, Germany
[4] Institute of Physics, Azerbaijan National Academy of Sciences, 370073 Baku, Azerbaijan

Received: February 03, 2008

Abstract. Confocal Raman Microscopy combines the three-dimensional optical resolution of confocal microscopy and the sensitivity to molecular vibrations which characterizes Raman spectroscopy. Hence, the technique is capable of providing a three-dimensional image of the chemical composition with micrometer resolution. An image is obtained by raster-scanning the sample with respect to the laser focus and measuring the integrated intensity of characteristic Raman lines. We present three applications of this method to different classes of materials. In specimens of sintered ceramics, the composition is determined and the size and shape of grains are visualized. Spider silk fibers show Raman spectra which are characteristic of the spider species; in some cases the fibers have hollow cores. Polymer fibers produced by electrospinning from mixtures of polymer solutions feature homogeneous Raman spectra, even in cases of immiscible polymers. This demonstrates that the electrospinning technique produces materials which are largery homogeneous on the micrometer length scale. The compositions of the fibers agree for most samples, but not in all cases, with the compositions of the solutions.

1. INTRODUCTION

Confocal microscopy is a technique which provides three-dimensional optical resolution on the order of the wavelength of light. In contrast to regular microscopy, the sample is not illuminated homogeneously within an extended field of view, but a Gaussian laser beam is tightly focused by a microscope objective to a diffraction-limited spot on the sample. Scattered or emitted light from this spot traveling in backward direction is collected and collimated by the same objective and then focused through a small pinhole onto a detector. An image is obtained by raster-scanning the sample with respect to the laser focus. The pinhole acts as a depth selector, since only light originating from the focal spot has its focus within the pinhole and can reach the detector. Light from other depths in the sample, above or below the focal plane, is not collimated by the objective and, as a consequence, will be defocused at the pinhole. Hence, out-of-focus sections do not contribute blurred signals but are dark.

The method was invented in 1955 and patented in 1961 by M. Minsky at the Massachusetts Institute of Technology (MIT) to avoid thin-slicing of brain tissue [1]. It became practical and found wide-

Corresponding author: Kerim R. Allakhverdiev, e-mail: kerim.allahverdi@mam.gov.tr

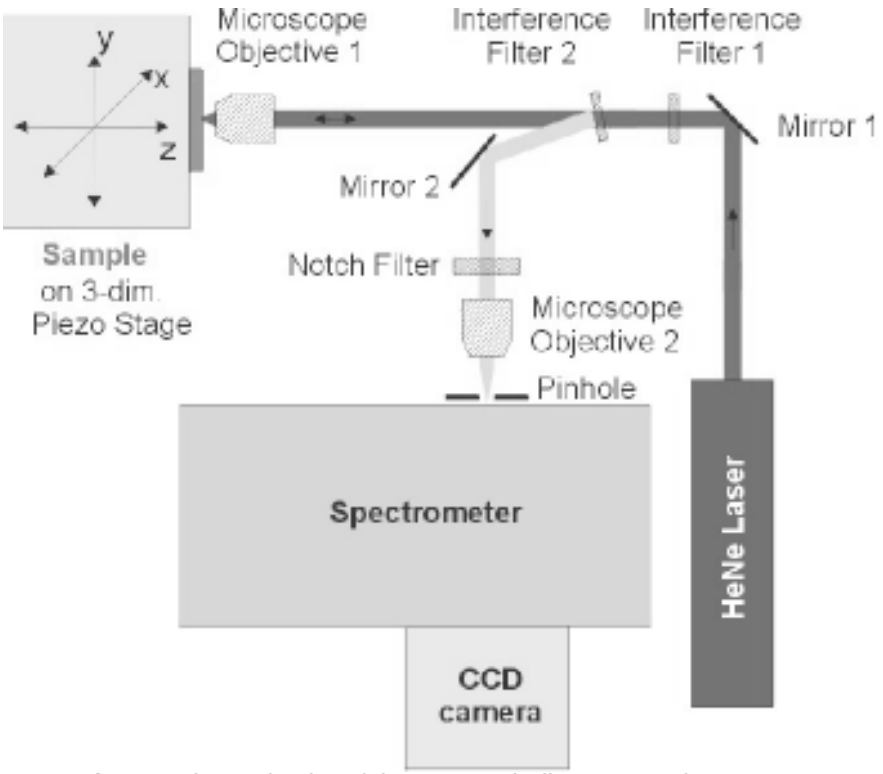

Fig. 1. Schematic plot of the custom-built Raman microscope.

spread use only much later, when lasers and cheap and powerful computers for experiment control and data acquisition were available. Today it is mainly applied in the life sciences.

Since in confocal microscopy only light from a diffraction-limited spot is recorded at a time, it can easily be combined with other techniques which perform a further analysis of the light signal, e.g., with respect to its spectral composition or time dependence. In this way confocal Raman, fluorescence, or fluorescence lifetime imaging microscopy (FLIM) [2] are obtained. In confocal Raman microscopy, the chemical composition of a sample can be imaged by recording the integrated intensity of characteristic Raman lines of the substances involved. Thus one can investigate, whether and to which degree mixtures of substances are homogeneous on the length scale of micrometers and above. It is easily possible, e.g., to map the composition of pharmaceutical products and to visualize the macro-phase separation of polymer mixtures [3]. A prerequisite for the applicability of the method is, however, that the fluorescence background must be sufficiently low in order not to bury the weak Raman signals. The spatial resolution achievable with confocal Raman microscopy in the lateral directions and along the light path is given by

$$\Delta x = \Delta y = 0.61\lambda / NA, \quad \Delta z = 0.89\lambda / (NA)^2,$$

where λ is the wavelength of light and *NA* is the numerical aperture of the microscope objective [1].

2. EXPERIMENTAL DETAILS

Although confocal Raman microscopes are commercially available, we used a custom-built apparatus because of its greater flexibility. It is sketched in Fig. 1.

Details of the set-up have been given elsewhere [3,4]. Briefly, the light source is an unpolarized HeNe laser with a wavelength of 632.8 nm. Its beam is sent through a plasma line filter and enters the side port of a modified inverted microscope Swift M 100 equipped with a semi-apochromat objective Leica PL FLUOTAR 100×/0.75. The laser power in the focus amounts to a few milliwatts. The scattered radiation collected and collimated by the objective

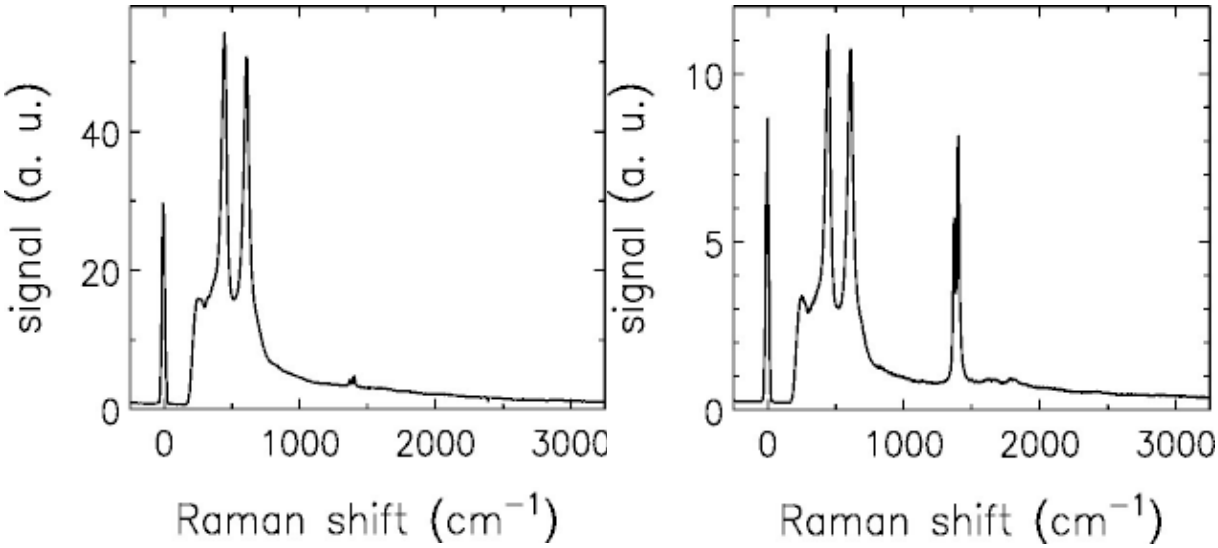

Fig. 2. Raman spectra of TiO_2 (left) and mixed TiO_2 / Al_2O_3 ceramics (right).

is separated from the incoming light path by a dichroic beam splitter (Chroma), passes through a holographic notch filter (Kaiser Optical Systems) for suppressing the Rayleigh line, and is focused into a 50 cm monochromator (Acton Research SpectraPro-500i), whose entrance slit has been replaced with an 80 μm pinhole for confocal depth selection. A grating of 300 grooves per millimeter was used. The spectra are recorded by a liquid-nitrogen-cooled CCD camera (Princeton Research, 1340 × 100 pixels) at the exit focal plane of the monochromator. The sample is moved with respect to the laser focus with a 3-d piezo translator (Piezosystem Jena, model TRITOR 102). The integration times of the Raman spectra varied between about 1 and 60 seconds, depending on the signal intensity. Images were usually recorded with 1 s integration time per point.

3. RESULTS AND DISCUSSION

3.1. Ceramics samples

Sintered ceramics samples of TiO_2 (rutile), α-Al_2O_3, and a mixture of both materials were prepared at the Materials Institute of the Marmara Research Centre of TÜBITAK, Gebze/Koçaeli, Turkey. They produce very strong Raman signals, as shown in Fig. 2.

The TiO_2 spectrum comprises lines below 800 cm^{-1}, that of Al_2O_3 is characterized by very intense and narrow lines around 1400 cm^{-1}. Due to the clear separation of the lines, it is very easy to map the spatial distributions of the two substances in a mixed sample. Fig. 3 shows an example of an impurity grain of alumina in a TiO_2 sample.

The images comprise an area of 10 × 10 μm; they were recorded with separations of each 2 μm in the depth direction. The integrated intensity of the alumina lines has been color-coded. The size and shape of the impurity grain and its three-dimensional orientation in space are well visible. One must note, however, that towards the bulk of the sample the *z* resolution deteriorates (bottom row of images in Fig. 3). This is due to the refraction at the surface, which elongates the focus with increasing depth in the sample [5,6]. The effect would be much less severe with the use of an oil immersion objective.

3.2. Spider silk fibers

Spider silk forms a class of remarkable biological materials, which combine high mechanical strength with very low weight. Some types of fibers carry droplets of a sticky fluid for capturing insects. Fig. 4 shows that the Raman spectra of fibers produced by different spider species can be very different, reflecting the differences in the protein composition.

The three-dimensional resolution of confocal Raman microscopy yields the possibility to investi-

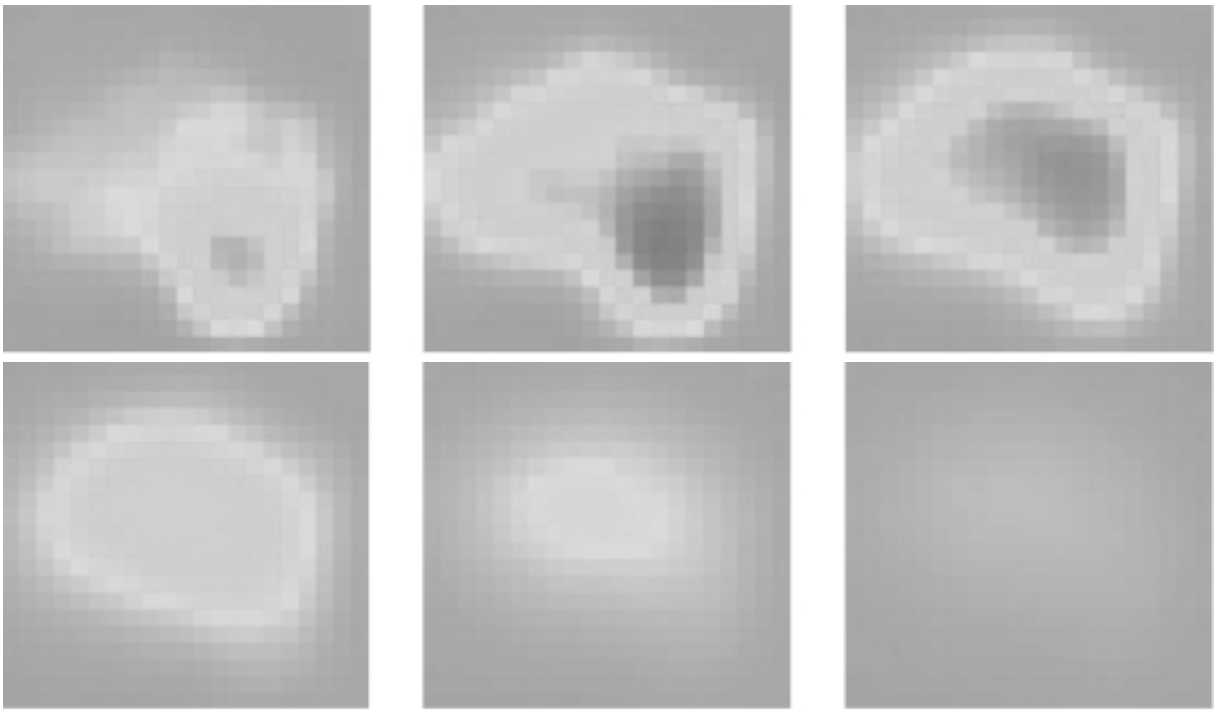

Fig. 3. Raman images of an Al_2O_3 impurity grain in a matrix of TiO_2. The field of view is 10 × 10 μm; successive images were recorded 2 μm apart in depth with the depth increasing from upper left to lower right. The amplitude of the integrated Al_2O_3 lines has been color-coded with blue corresponding to high and red to low signal strength.

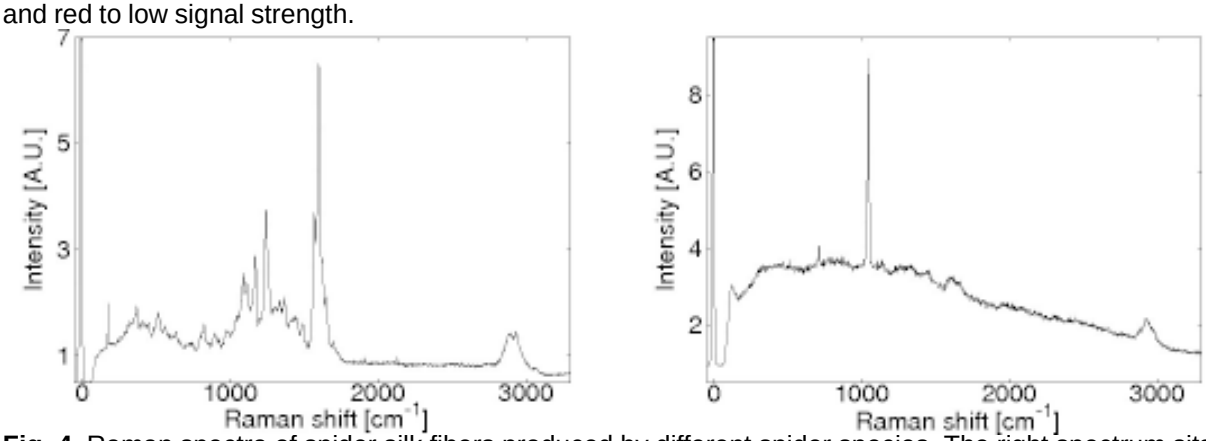

Fig. 4. Raman spectra of spider silk fibers produced by different spider species. The right spectrum sits on top of a moderate fluorescence background.

gate the cross section of the fibers by *x-y* scans. Fig. 5 demonstrates that also here dramatic differences show up.

The fiber in the left image is approximately 6 μm in diameter and clearly has a hollow core. Its wall thickness is at most 1 μm. The other fiber is much thinner – between 1 and 2 μm – and appears to be compact. The elongated shapes of the fibers are not real, but are again mainly caused by the effects of surface refraction [5,6]. More detailed and systematic investigations of spider silk fibers by confocal Raman imaging may reveal other shapes and may help establish a relationship between the composition and cross section of a fiber and its function in the spider web.

3.3. Electrospun fibers from polymer blends

Electrospinning is a technique which produces continuous fibers from a polymer solution or melt, through the action of an electrical field [7]. A typi-

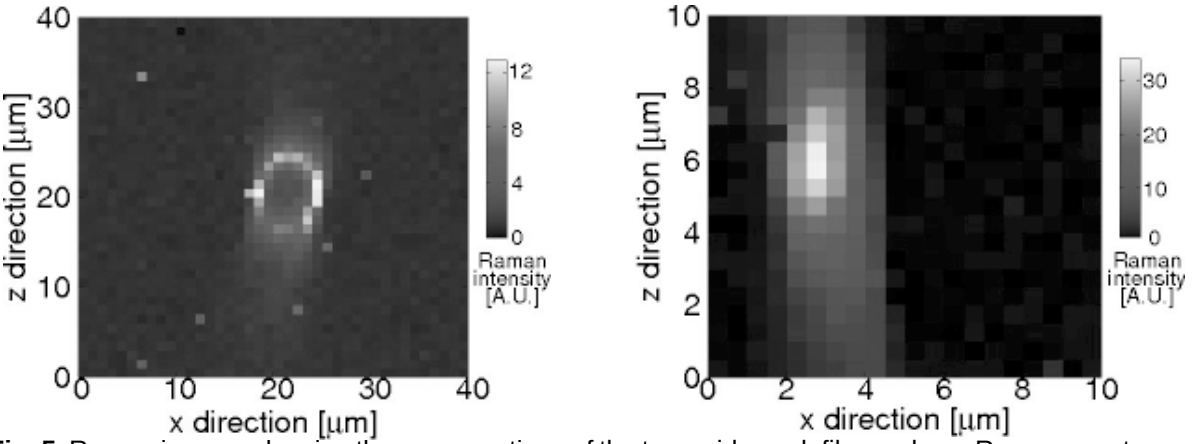

Fig. 5. Raman images showing the cross sections of the two spider web fibers whose Raman spectra are plotted in Fig. 4. The integrated intensities of the strong Raman lines at 1600 cm^{-1} (left) and 1048 cm^{-1} (right), respectively, are shown in a color-coded representation.

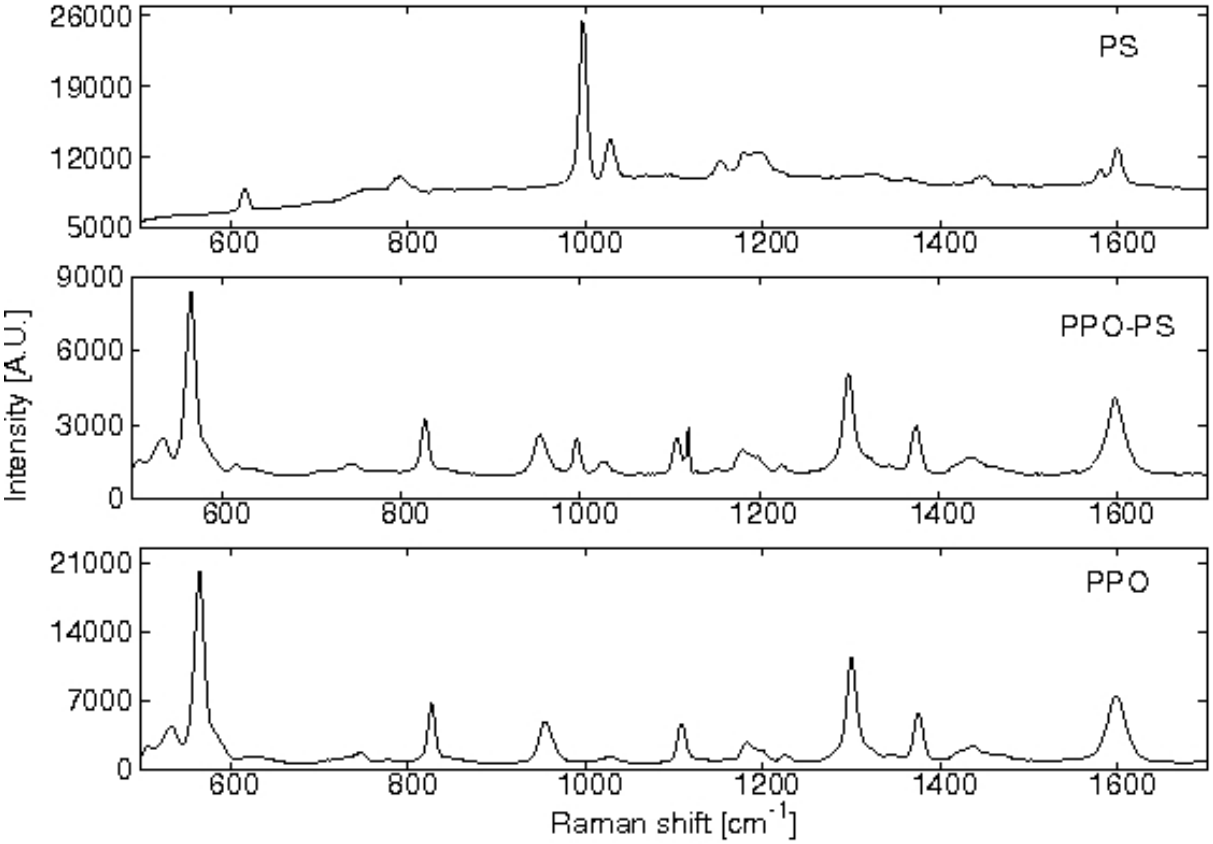

Fig. 6. Part of the Raman spectra of polystyrene (PS; top), polyphenylene oxide (PPO; bottom), and an electrospun fiber produced from a mixed solution (25:75) of the two polymers. The composition of the fiber, as estimated from the intensities of characteristic Raman lines, is similar to that of the solution.

cal experimental set-up consists of a syringe containing the polymer solution, a high-voltage supply, and a collector. When the electric potential applied to the solution is high enough to overcome the surface tension of the liquid, a charged jet is ejected. During its travel, the jet is elongated several thousand times and the solvent evaporates, leaving solidified polymer filaments in the form of a nonwoven fabric on the collector. These electrospun fibers with diameters on the order of nano- to mi-

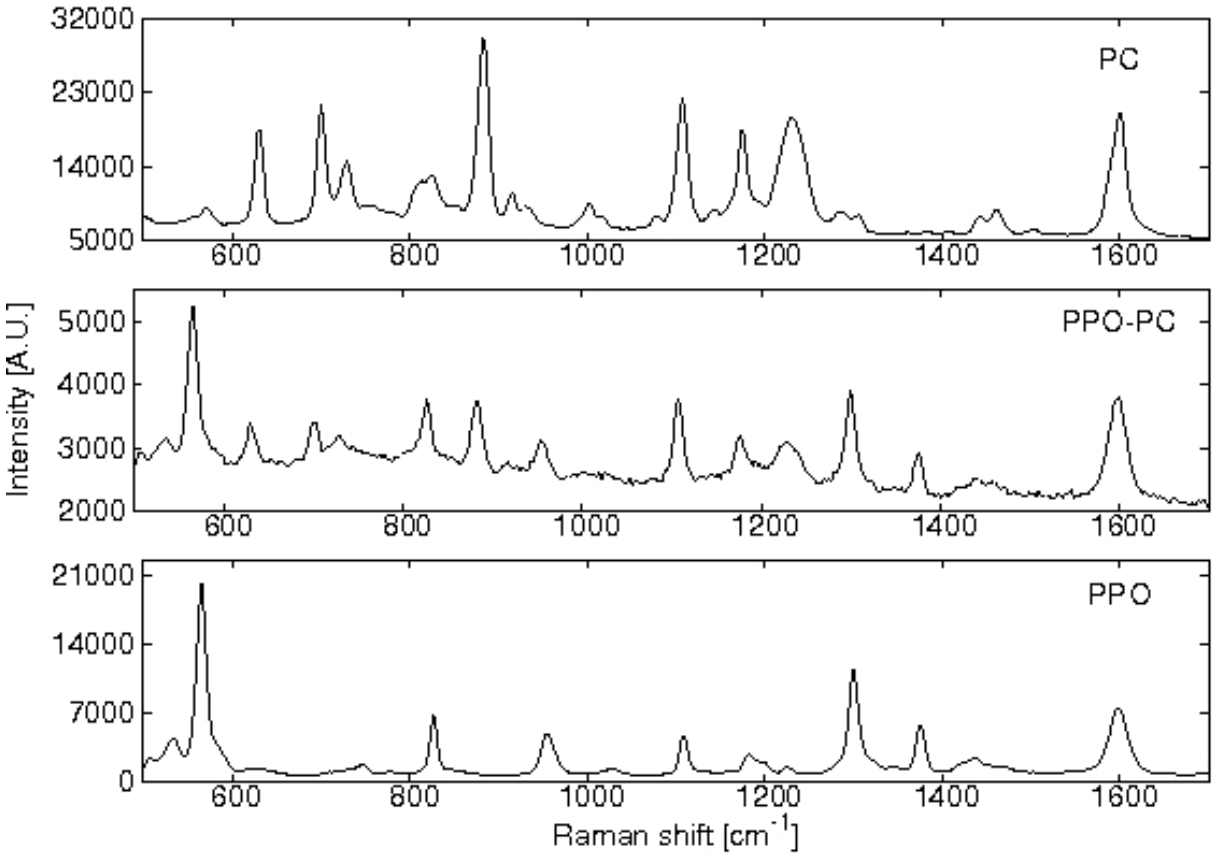

Fig. 7. Same as Fig. 6 for a mixture of polycarbonate (PC) and polyphenylene oxide (PPO). The composition of the solution was 50:50, the fiber contains relatively more PPO.

crometers and high surface area to volume ratios find applications in multiple fields such as filtration, protective clothing, medicine, and electronics [8].

Polymer blending is a simple and widely used technique for combining the properties of two or more polymers in one material. Electrospinning of polymer blends allows the creation of advanced materials, as functionalities are combined and special internal and surface morphologies of the fibers can be developed. Since most of the polymer blends are immiscible, usually phase separation occurs during their processing. In electrospinning, however, the evaporation of the solvent occurs very quickly, so that coarse phase separation upon solidification is very much hindered [9].

By the characterization of the phase morphology, the scale of the phase separation and the composition of the fibers can be determined. Because of the small diameter of electrospun fibers, techniques such as TEM and AFM are often required for their morphological characterization, but sample preparation usually involves the isolation of single fibers as well as the etching or staining of one of the components, which can be tedious and complicated.

In this paper, we demonstrate the possibility of using confocal Raman microscopy for analyzing the structure of electrospun fibers. To this end, a miscible blend consisting of polyphenylene oxide (PPO) and polystyrene (PS) and an immiscible blend of PPO/polycarbonate (PC) were electrospun from chloroform solutions. The Raman spectra obtained from the fibers are compared with those of the pure components in Figs. 6 and 7.

Since the characteristic lines are located between 500 and 1700 cm^{-1}, only this region has been plotted. For both blends, the spectra show that both polymer constituents are present in the same volume element of each fiber. This result has been expected in the case of the miscible system PPO/PS. The homogeneity found in the fiber of the immiscible blend PPO/PC, however, is surprising and

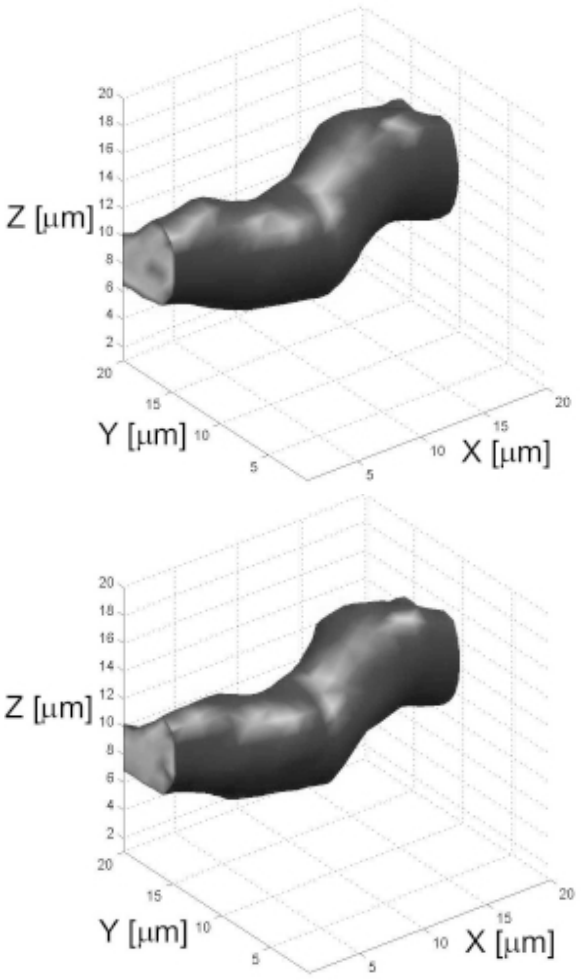

Fig. 8. Three-dimensional Raman images of an electrospun PPO/PC fiber showing the spatial distributions of PPO (top) and PC (bottom), respectively, in false-color representation. The field of view comprises 20 mm in μll three directions of space.

reveals the potential of electrospinning to suppress macro-scale separation. If phase separation takes place, it must be restricted to much smaller length scales in the nanometer range. In this case, fine morphologies can be formed consisting of one phase dispersed in the other, the two phases interpenetrated (co-continuous), or a core-shell structure.

The 3-d Raman mapping of a PPO/PC fiber shown in Fig. 8 confirms the above result, since the spatial distributions of both polymers coincide perfectly. Moreover, the homogeneity of the blend composition within the fiber mat could be determined by the evaluation of different spots of it. The spectra did not show strong variations.

The composition of the fibers in the focal spot can be estimated from the relative intensities of characteristic Raman lines. In most samples it was found to agree approximately with the composition of the mixed polymer solutions. Some samples of both the PPO/PS and the PPO/PC system, however, showed clear deviations. For instance, the fiber whose Raman spectrum is plotted in Fig. 7 clearly contains more PPO than PC, although the composition of the solution was 50:50. Blend composition and the solubility in the electrospinning solvent are important factors which affect the development of the fiber morphology. Since both the miscible and the non-miscible system showed these deviations, one possible explanation might be that some phase separation occurred within the polymer solution prior to the electrospinning and a gradient of blend compositions was, therefore, obtained. Further investigations are necessary to clarify this point.

4.CONCLUSIONS

We have demonstrated three applications of confocal Raman microscopy in the fields of materials science and biology. The size and shape of impurity grains of Al_2O_3 in a sample of sintered TiO_2 ceramics were investigated. Due to the strong Raman signals of the two materials and their different spectra it is very easy to detect the impurity grains. The Raman spectra and cross sections of spider silk fibers produced by two different species were measured. Both the spectra and the cross sections show pronounced differences. One of the fibers, which is about 6 μm thick, was found to have a hollow core and a wall thickness of at most 1 μm. The most interesting and unexpected result was obtained on polymer fibers produced by electrospinning. The compositions of all investigated fibers turned out to be very homogeneous on the micrometer scale, even if they were prepared from solutions of non-miscible polymers. The mechanism causing this effect will be the subject of future research.

ACKNOWLEDGEMENTS

Financial support from the German Research Foundation (DFG), the Emil-Warburg-Stiftung, Bayreuth, the Scientific and Technological Research Council of Turkey (TÜBITAK), and the Turkish State Planning Organization (DPT) is gratefully acknowledged.

REFERENCES

[1] *Confocal Microscopy,* ed. by T. Wilson (Academic Press, London, 1990).
[2] M.J. Booth and T. Wilson // *J. Microsc.* **214** (2004) 36.
[3] L. Kador, T. Schittkowski, M. Bauer and Y. Fan // *Appl. Opt.* **40** (2001) 4965.
[4] C. Pérez León, L. Kador, K.R. Allakhverdiev, T. Baykara and A.A. Kaya // *J. Appl. Phys.* **98** (2005) 103103.
[5] N.J. Everall // *Appl. Spectrosc.* **54** (2000) 773.
[6] K.J. Baldwin and D.N.Batchelder // *Appl. Spectrosc.* **55** (2001) 517.
[7] J. Doshi and D.H. Reneker // *J. Electros.* **35** (1995) 151.
[8] A. Greiner and J.H. Wendorff // *Angew. Chem. Int. Ed.* **46** (2007) 2.
[9] M. Bognitzki, T. Frese, M. Steinhart, A. Greiner and J.H. Wendorff // *Polym. Eng. Sci.* **41** (2001) 982.